Office of Naval Research
Department of the Navy
Contract Nonr-220(43)

AN EXPERIMENT CONCERNING PARTLY CLOSED CAVITIES BEHIND A SURFACE-PIERCING ROD

by
M. C. Meijer

Hydrodynamics Laboratory
Kármán Laboratory of Fluid Mechanics and Jet Propulsion
California Institute of Technology
Pasadena, California

Report No. E-110.1

January 1964

Department of the Navy
Office of Naval Research
Contract Nonr-220(43)

AN EXPERIMENT CONCERNING PARTLY CLOSED CAVITIES BEHIND A SURFACE-PIERCING ROD

by
M. C. Meijer

Hydrodynamics Laboratory
Karman Laboratory of Fluid Mechanics and Jet Propulsion
California Institute of Technology
Pasadena, California

Report No. E-110.1 January 1964

AN EXPERIMENT CONCERNING PARTLY CLOSED CAVITIES BEHIND A SURFACE-PIERCING ROD

by

M. C. Meijer*

California Institute of Technology
Pasadena, California

1. Introduction

Thomsen in Ref. (1)** emphasizes three different states of ventilation occurring at surface-piercing rods, as observed by Hay (2). Hay has towed cylindrical rods which intersect the water surface, at different speeds and at different depths of submergence. From his photographic records, the following observations have been made.

At relatively low speeds, an air filled cavity is formed in the wake of the rod, which is open to atmosphere and which extends downwards to a point above the base of the rod. With increasing speed, this point moves downward towards the base of the rod. This form of cavity has been called the "Pre-Base Ventilation State".

After the cavity has reached the base, the state was referred to as the "Base Ventilation State", which is found to persist with further increased speed.

---

* Senior Research Engineer, Hydrodynamics Laboratory, California Institute of Technology; on leave from the Technological University of Delft, Holland.

** Numbers in brackets refer to the references at the end of the text.

After the speed was increased over a certain level, the size of the cavity was observed to decrease again forming a cavity closed at the water surface. In this case the state was called the "Post-Base Ventilation State".

Since this last phase in the development of the air-cavity has not been observed in the Free Surface Water Tunnel at the California Institute of Technology, it was thought desirable to perform some experiments in order to find the conditions under which this Post-Base Ventilation State can occur.

The present results are to be regarded as preliminary. A full explanation of the ventilation phenomena described in the references above and the text of this report to follow is not yet available. Nevertheless, since the results of the present work are at variance with published work, it was thought worthwhile to present them now. Hopefully a more thorough understanding of the ventilation phenomena will be obtained in the not too distant future.

2. Preliminary Considerations

After reading Thomsen's report, the author considered the possibility that the differences between the ventilation states may be caused by specific differences in flow conditions which seem to appear in a towing tank and in a water tunnel. Especially turbulence, surface tension and vibration were thought of as possibly responsible for the difference in behavior at the water surface.

As compared to the Free Surface Water Tunnel, which has no honeycomb and hardly any settling chamber, the turbulence level in a

towing tank must be relatively very low.

With respect to the surface tension properties of the water, it can be noted that dust may be floating on the surface of the towing tank, whereas particles in the tunnel will be distributed homogeneously. Vibrations of the rod may be mainly structural from the carriage in the towing tank case and mainly of hydrodynamic origin in the tunnel.

Considering the differences mentioned above, it might be speculated that in the towing tank, closure of the cavity at the water surface will be more readily achieved than in the Free Surface Water Tunnel.

3. Apparatus

The models were fixed to the 3-component strain gage balance which has been installed for the Free Surface Water Tunnel; no drag measurements were performed though, as the sensitivity of the balance (range: 25 lbs.) proved to be too small during the main part of the experiments.

In order to facilitate the comparison on the different cavity forms, a grid divided in tenths of half inches was reflected into the plane of the cavity with the aid of an inclined glass plate at 45 degrees in front of the tunnel window.

Photographs were taken through the glass plate. The exposure was 1/25 of a second at F/7.7 on 250 A. S. A. "Royal Pan" film. The lighting was supplied by three 750 watt lamps at a distance of $3\frac{1}{2}$ feet from their respective objects, one spotlight pointed at the grid and one at the cavity, the last one from beneath and slightly downstream in the centerplane of the tunnel. One lamp with separate diffusing reflector from

downstream behind the tunnel was used to light the model (see Fig. 1).

4. Experimental Procedure

4.1 In the first experiment a 5/16 inch rod (8mm) was used piercing the surface at a velocity of about 12 f. p. s. (3. 7 m/sec). The depth of submergence was about H = 5 inches (127mm). According to Fig. 14 of Ref. 1, the post-base ventilation state would be expected to occur. Instead, the cavity was quite open at the top. With the hand or a flat plate covering the cavity, parallel to and near the free surface, the cavity could be closed partially. In this case the flow at the surface changed suddenly, which could be felt, as upward pressure on the means of closure changed into suction. Air was heard to be sucked through a small opening between the cover and the rod. After removal of the artificial closure, this condition could persist for some time, but would soon change again into the open base ventilation state. Total covering of the surface behind the rod resulted in the entire disappearance of the cavity, which would always reappear when the cover was removed. Whether or not the disturbances due to the free stream turbulence are responsible for this reappearance at this low Froude number is not known.

In this preliminary experiment no measurements or photographs were made. The Reynolds number based on the rod diameter was of the order of 3×10^4. The same observations have been made with a 1/8 inch rod submerged to 3-5/8 inch depth. The extreme velocity in this case was 20. 75 feet per second.

4.2 In order to obtain subcritical flow conditions with respect to the

Reynolds number comparable to those in Hay's experiments, a rod with a diameter of 1/8 inch (3 mm) was selected and the tunnel was run at a velocity of 3.94 ft./sec. (1.2 m/sec.). Now the Reynolds number was about 3.8×10^3. The tunnel velocity was too low for proper supercritical operation, (now with respect to the channel Froude number) but as the actual and local water surface was measured, the velocity, as calculated,was considered to be approximately correct, although it should be noted that some change of velocity near the surface must have been present due to some curvature of the surface then.

The ventilation state in this experiment was varied by changing the submergence depth of the rod. At a depth of about 0.138 ft. (42 mm) a transient condition occurred in which the form of the cavity changed considerably and generally at a slow pace with time as discussed in the next section.

4.3 With a 1/4 inch rod (~6.3 mm) a transient condition was found with a velocity of 5.44 ft./sec. (1.66 m/sec.), the Reynolds number being about 1×10^4. In this case the changing of form was much more abrupt, and to photograph the different forms of the cavity, the submergence depth had to be adjusted. With the lower velocity of 4 ft./sec. (1.22 m/sec.) again a more stable transition form was obtained.

5. Analysis of Data

5.1 The process of the change of form mentioned in 4.2 can be described as shown in the photographs of Fig. 3. Photograph 2 shows the open form obtained after shaking of the rod in the direction of the flow. The length of the cavity just below the water surface may vary some-

what, depending upon the intensity of the shaking procedure. In the region of the extremity of the cavity downstream, near the water surface, a small indication of a re-entrant jet exists, seen in the side elevation of the cavity.

This open condition may persist for some time, but then the cavity slowly becomes shorter and the "re-entrant jet" becomes a small "bay", as shown in photograph 6 (also in 1 and 7). The "bay" seems to proceed along a definite curve which is independent of the submergence depth. (Photographs 5 and 9).

When the "bay" reaches the rod, the cavity is cut in two. Presumably, because of surface tension effects, a third bubble is formed in between, and thin films of water may divide the lower and upper bubbles, however, not interfering with the general shape of the cavity in these instances (see photograph 3).

It must be noted, that surface tension will play a role in this case where the dimensions and hydrodynamic forces are small.

If the end of the rod is too far away, as is the case in photographs 8, 9, and 10, the closure between the bubbles will be complete and the lower bubble will disappear (photograph 10). In the case of photograph 3, the presence of the end of the rod seems to promote the leakage of air from the top bubble into the lower one.

The most stable form of the series seems to be that of photograph 4, which occurs after the lower boundary of the upper bubble and the upper boundary of the lower bubble have merged into each other, which occurs suddenly. In this case the two bubbles remain separated by a

film of water, the length of the cavity just below the water surface becomes shorter and, what is the most remarkable feature, the lower end of the upper bubble forms a "flag" of a rough texture, which always extends from a line about vertical through the end of the lower bubble, to the curve of the original open cavity (photograph 2). All the forms in the photographs numbered 3 through 6 remain within the boundary of the open form and the curvature near the end of the rod remains approximately the same. The length of the top of the cavity only changes considerably at the last instant (photograph 4).

When the submergence depth is reduced, only a small "bay" is formed as is shown in photograph 7, after which the form remains the same. With a larger submergence depth, the lower bubble disappears, as is mentioned earlier. In photographs 8 and 9, the length of the cavity near the surface appears to be larger than was the case in the previous series, but this may be caused by the amount of shaking applied.

In the case of photograph 10, where the lower cavity has disappeared, the lower end of the remaining cavity is situated at exactly the same place as the division of the bubbles in photograph 10 (and 11) it is also noted that the streamlines at the lower boundary of a remaining upper-cavity are headed downwards.

5.2 Being acquainted with the proceedings described above, it is possible to guess the same general configuration at higher Reynolds numbers, photographed in 12 and 13 for the thin rod and 14 through 18 for the 1/4 inch rod. In the case of the longer rod, the curve (see Fig. 2) along

which the "bay" proceeds seems to have moved downwards with the end of the rod; where the rod is thicker, the curve may have been moved upward, even above the free water surface.

In the case of photograph 18 the rear boundary of the lower bubble curls inwards and forms the separate bubble which can be seen within the top of the cavity attached to the rod.

5.3 The cavity shown in photograph 11 is of interest because of its separations. In this case the submergence depth is large; the end never carried a cavity. The position of the vertical separation film in the cavity is quite stable. The bubbles behind this line can be entrained by the flow, leaving the forward cavity unaltered. This may be important, as in the experiments described under 4.1 it was already observed that the length of the cavity, after opening of the water surface changed in steps rather than continuously.

5.4 About photograph 15, it is noted that during this series the submergence depth was mechanically limited to 0.304 ft., in which range it proved to be impossible to make the lower cavity disappear. Photograph 15 now was obtained with a turbulence stimulating rod of 1/8 inch diameter which was held at a 2 foot distance upstream of the model.

5.5 Concerning the form of the cavity at the intersection with the water surface, the following remarks can be made:

At relatively low Reynolds numbers, the surface appears to be partly closed all the time. Even in the case of photograph 2 it is probable that a small pressure drop at the air-entrance existed. Only in the case of photograph 17 is it certain that the surface is entirely open.

The hypothesis can be made that this is caused by the position of the curve of the "bay-points" being above the water surface.

6. Comment on Thomsen's Diagram

In Fig. 4 of Ref. 1, Thomsen showed the dependency of the flow states from the ratio d/H, the inverted square of the Froude number gH/U^2 and Reynolds number Re based on the diameter.

The symbols used are:

d = diameter
H = depth of submergence
g = acceleration of gravity
U = velocity

This diagram has been reproduced at the same scale in Fig. 4 of this report. Hay's experimental points have been replaced by points representing the photographs of Fig. 3 and one extreme condition.

It is thought, that replacement of gH/U^2 by its inverted value, i.e. U^2/gH, makes a better picture. In Fig. 5 d/H has been plotted against U^2/gH. The black dots represent the experimental data reported here; the open symbols are taken from Thomsen's diagram and indicate the onset of the post-base ventilation state. The dot at the extreme right of the diagram shows the extreme condition, at which still no post-base ventilation state could be obtained in a natural way.

The approximate linearity of the average transition line between the base- and post-base ventilation state, as derived from Hay's experiments, indicate that this phenomenon is little dependent of the submergence depth H, which seems to be valid also where d/H = 1. It can hardly be plausible, that this is related to the underwater flow. This

seems to point at influences above the surface, such as the increase of the height of the spray sheet with increasing speed, which should be proportional to U^2.

If such a spray sheet makes contact with a plate or other cover, parallel to the water surface, than it has been shown that the cavity obtains a shape in agreement with the description of the post-base ventilation state.

7. Conclusions

Although experiments have been made at very low values of gH/U^2 and low values of d/H, the post-base ventilation state, as described by Thomsen, did not occur in the Free Surface Water Tunnel in a natural manner. It could be obtained by partial closure of the gap in the water surface with a plate. Removal of this plate resulted always in a restoration of the original base ventilated state if the velocity was high enough.

It seems reasonable to suppose that in the case of Hay's experiments such a plate or other spray cover near the surface must have been present, which became effective at high velocities, when the spray sheet could make good contact with it. At the transition of the pre-base ventilation state and the base ventilation state, stable cavities did exist which were nearly closed near the water surface, or at a lower point.

REFERENCES

1. Thomsen, P., "Cavity Shape and Drag in Ventilated Flow; Theory and Experiment", TRG, Inc. Report 156 SR-2, 2 Aerial Way, Syosset, New York, February, 1963.
2. Hay, A. D., "Flow About Semi-Submerged Cylinders of Finite Length", Princeton University, October 1, 1947.

ACKNOWLEDGMENT

The author is indebted to the University of Technology of Delft, the Netherlands, to "The Netherlands Organization for the Advancement of Pure Research, "Z. W. O.", which supported his visit to the California Institute of Technology, and to the personnel of the Institute who assisted him when it was needed.

This work was supported by the U. S. Office of Naval Research under Contract Nonr-220(43).

APPENDIX I

Data Sheet

Rod d = $\frac{1}{8}$ inch, position vertical.

Water level at rest above bottom F. S. W. T. = 1.434 ft. at which the model raising mechanism is set with the end of the rod touching the water surface.

Grid reflection in optical plane under water of rod, divisions are in 1/10 of 1/2 inch.

Drag readings are of the same magnitude as the drift of the apparatus.

Barometer reading: 29.4 inch Mercury at 72° F.

Camera setting: 1/25 sec. F/7.7.

Film sensitivity: 250 A. S. A.

Lighting: 1 spotlight 750 W, distance: $3\frac{1}{2}$', directed at grid.

1 spotlight 750 W, distance: $3\frac{1}{2}$', directed at rear end of cavity from underneath and downstream.

Number of Picture	Velocity Reading	Water Level Above Bottom	Rod-End Level	Remarks
	Feet	Feet	Feet	
1	1.595	1.311	1.183	trial for exposure data
2	1.565	1.322	1.184	long cavity after shaking of rod; sometimes natural condition
3	1.565	1.322	1.184	natural condition, rear end of top cavity often with bubbles
4	1.565	1.322	1.184	
5	1.565	1.322	1.184	less stable
6	1.565	1.322	1.184	more stable

APPENDIX I

Data Sheet (continued)

Rod d = $\frac{1}{4}$ inch, position vertical

Number of Picture	Velocity Reading	Water Level Above Bottom	Rod-End Level	Remarks
	Feet	Feet	Feet	
7	1.565	1.322	1.205	only stable condition
8	1.565	1.322	1.170	after longitudinal shaking
9	1.565	1.322	1.170	less stable
10	1.565	1.322	1.170	stable
11	1.565	1.322	0.988	only stable form apart from rear end bubbles
12	1.690	1.229	0.964	just changing form
13	1.690	1.229	0.964	
14	1.698	1.235	0.954	transition
15	1.698	1.235	0.931	with aid of turbulence rod $\frac{1}{8}$" at 2 ft upstream
16	1.700	1.235	0.985	quite stable, transition
17	1.700	1.235	1.007	very stable
18	1.573	1.322	1.159	

APPENDIX II

Calculation of velocity and submerged height of rod, $\frac{d}{H}$ and $\frac{gH}{U^2}$

Barometer not corrected: 29.4 inch Hg at 72° F.

Rod diameter $d = \frac{1}{8}$ inch = 0.0032 m

Photograph No.	1	2-6	7	8-10	11	12-13
Vel. reading in ft. H_2O	1.595	1.565	same	same	same	1.690
Local water level in ft.	1.311	1.322				1.229
Vel. head in ft. H_2O	0.284	0.243				0.461
$\frac{1}{2}\rho U^2$ in kg / m^2	86.5	74.0				140.4
U^2 in $(m/sec.)^2$	1.69	1.45	1.45	1.45	1.45	2.75
U in m/sec.	1.30	1.20	1.20	1.20	1.20	1.66
U in f.p.s.	4.26	3.94	3.94	3.94	3.94	5.44
Local water level in ft.	1.311	1.322	1.322	1.322	1.322	1.229
Level of rod base in ft.	1.183	1.184	1.205	1.170	0.988	0.964
Submerged ht. in ft.	0.128	0.138	0.117	0.152	0.334	0.265
Same in m (H)	0.0390	0.0420	0.0305	0.0463	0.1017	0.0807
d/H	0.082	0.076	0.105	0.069	0.031	0.040
gH/U^2	0.227	0.284	0.206	0.313	0.688	0.288
$Re = Ud/\nu$	3.8×10^3	3.5×10^3	3.5×10^3	3.5×10^3	3.5×10^3	4.8×10^3

APPENDIX II
(continued)

Rod diameter $d = \frac{1}{4}$ inch = 0.0063 m d = 0.0032m

Photograph No.	14	15	16	17	18	Extreme U
Vel. reading in ft. H_2O	1.698	same	same	same	1.573	8.400
Local water level in ft.	1.235				1.322	1.650
Vel. head in ft. H_2O	0.463				0.251	6.750
$\frac{1}{2}\rho U^2$ in kg/m^2	141.0				76.5	2057.4
U^2 in $(m/sec.)^2$	2.76	2.76	2.76	2.76	1.50	40.42
U in m/sec.	1.66	1.66	1.66	1.66	1.22	6.36
U in f.p.s.	5.44	5.44	5.44	5.44	4.00	20.87
Local water level in ft.	1.235	1.235	1.235	1.235	1.322	1.650
Level of rod base in ft.	0.954	0.931	0.985	1.007	1.159	1.337
Submerged ht. in ft.	0.281	0.304	0.250	0.228	0.163	0.313
Same in m (H)	0.0856	0.0926	0.0761	0.0695	0.0497	0.0954
d/H	0.074	0.068	0.083	0.091	0.127	0.034
gH/U^2	0.304	0.329	0.271	0.247	0.325	0.023
$Re = Ud/\nu$	9.5×10^3	9.5×10^3	9.5×10^3	9.5×10^3	7.0×10^3	1.85×10^4

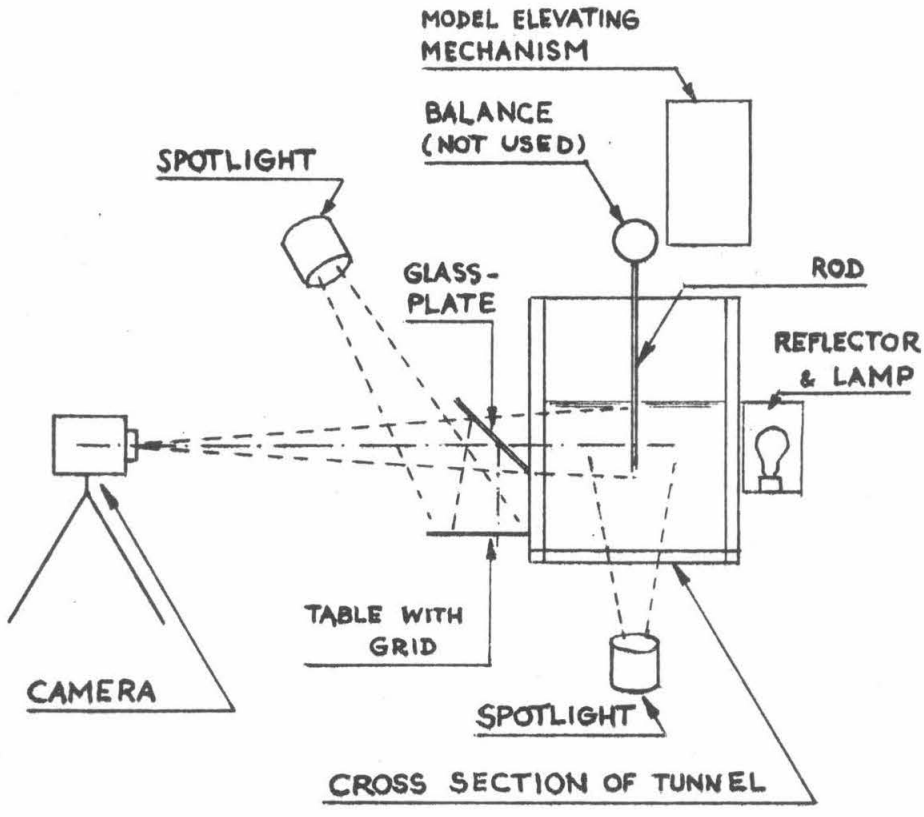

Fig. 1, Schematic Arrangement of Test Equipment

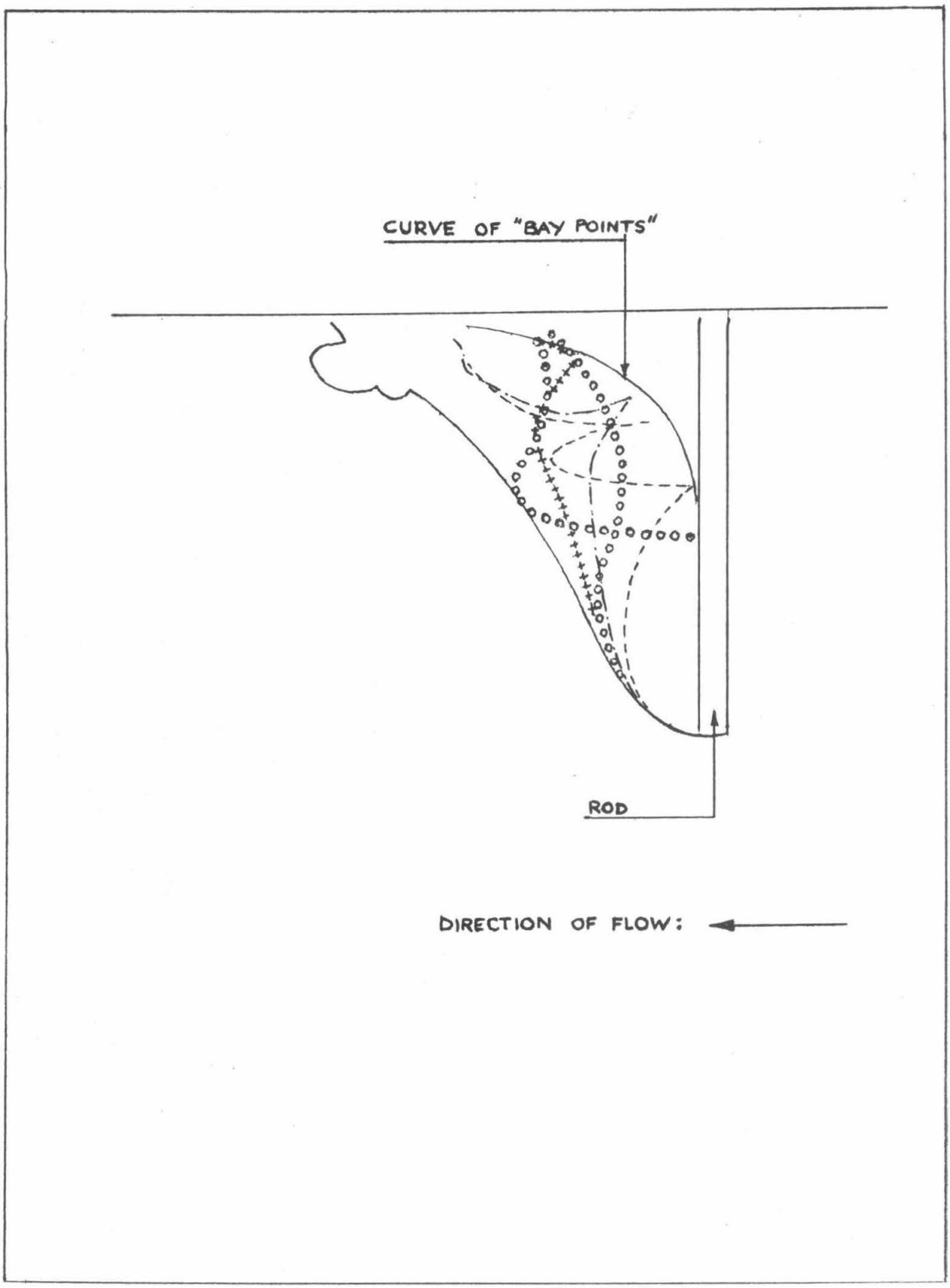

Fig. 2, Sketches of Photographs 2 through 6 Superimposed.

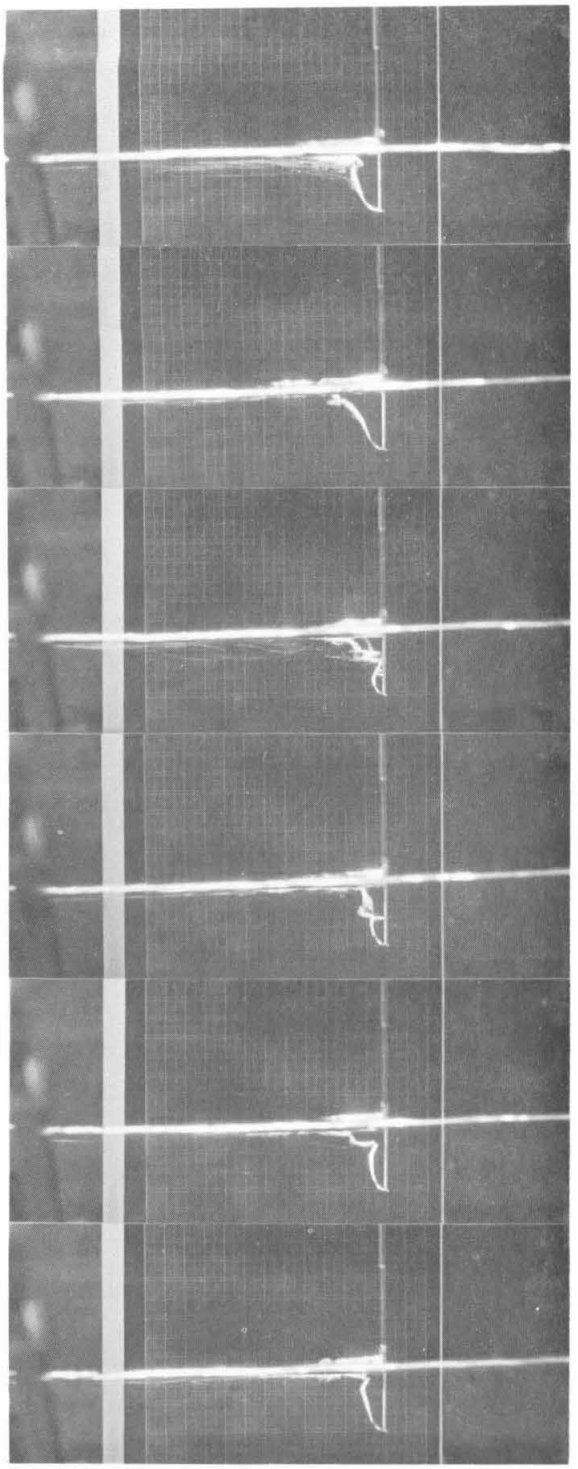

1. d = $\frac{1}{8}$ in. = 3.2 mm
   U = 4.26 f. p. s. = 1.30 m/sec
   H = 0.128 ft = 39.0 mm

2. After shaking of rod
   d = $\frac{1}{8}$ in. = 3.2 mm
   U = 3.94 f. p. s. = 1.20 m/sec
   H = 0.138 ft = 42.0 mm

3. Developed from 2, same data

4. Same as 3

5. Same as 3, unstable transient form

6. Same as 3

Fig. 3 Photographs of Rod in Water Tunnel. The flow is from right to left. In each case the diameter of the rod d, speed of water U and depth of rod H is listed. The ambient pressure was 29.1 in. Hg (9.800 kg/m^2) at 72°F (20°C). The large grid squares are one half of an inch on a side.

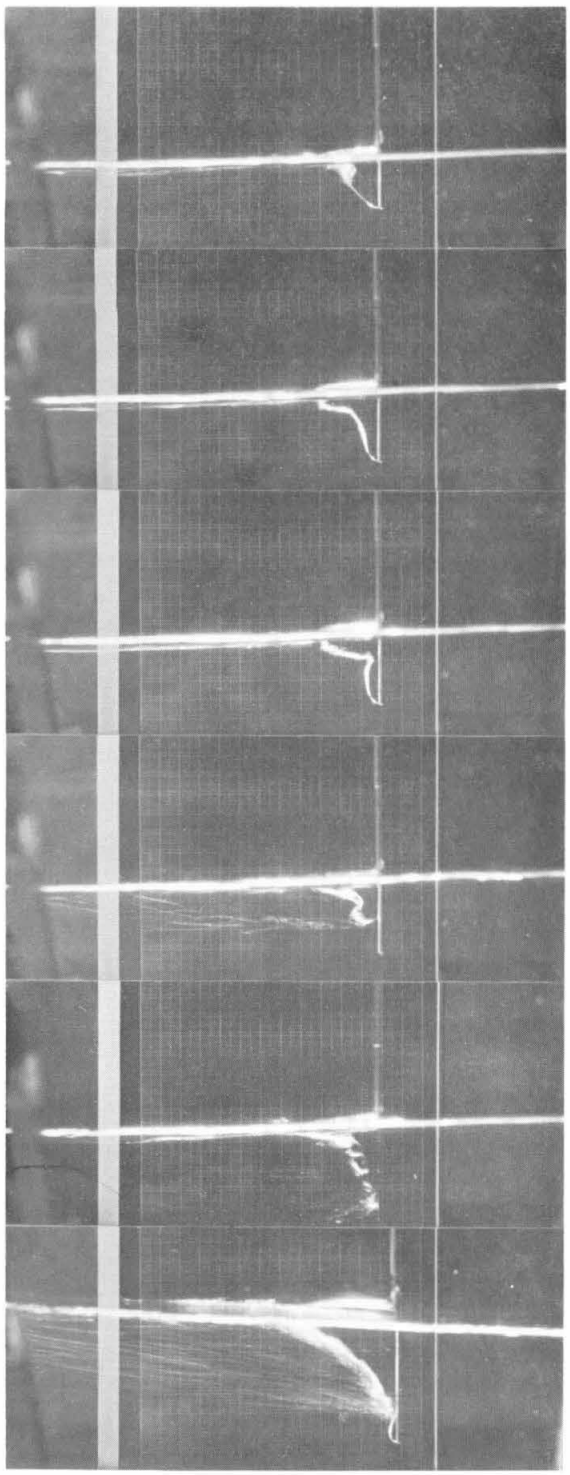

7. d = $\frac{1}{8}$ in. = 3.2 mm
   U = 3.94 f.p.s. = 1.20 m/sec
   H = 0.117 ft = 30.5 mm

8. After shaking of rod, not stable
   d = $\frac{1}{8}$ in. = 3.2 mm
   U = 3.94 f.p.s. = 1.20 m/sec
   H = 0.152 ft = 46.3 mm

9. Developed from 8, transient, same data

10. Same as 9, stable

11. Stable, with or without bubbles
    d = $\frac{1}{8}$ in. = 3.2 mm
    U = 3.94 f.p.s = 1.20 m/sec
    H = 0.334 ft = 101.7 mm

12. Form changing
    d = $\frac{1}{8}$ in. = 3.2 mm
    U = 5.44 f.p.s. = 1.66 m/sec
    H = 0.265 ft = 80.7 mm

Fig. 3 continued

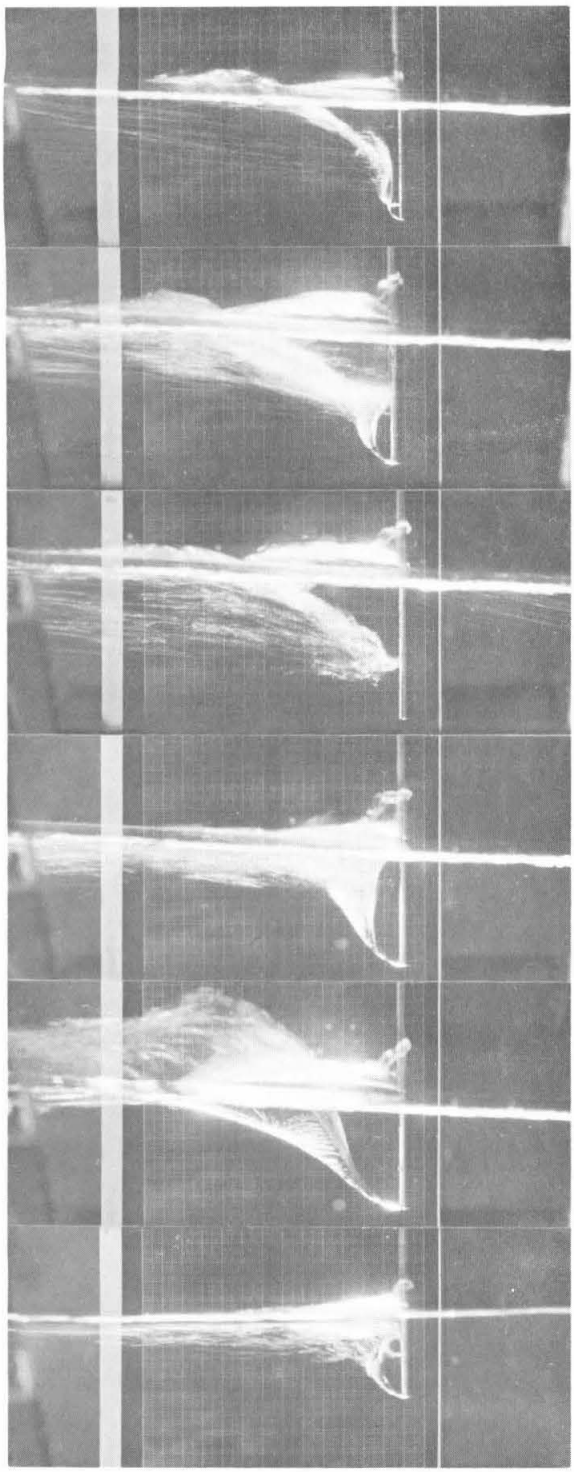

13. Same as 12

14. d = $\frac{1}{4}$ in. = 6.3 mm
U = 5.44 f.p.s. = 1.66 m/sec
H = 0.281 ft = 85.6 mm

15. With the aid of a turbulence rod $\frac{1}{8}$ in. dia., 2 ft upstream
d = $\frac{1}{4}$ in. = 6.3 mm
U = 5.44 f.p.s. = 1.66 m/sec
H = 0.304 ft = 92.6 mm

16. Transition form
d = $\frac{1}{4}$ in. = 6.3 mm
U = 5.44 f.p.s. = 1.66 m/sec
H = 0.250 ft = 76.1 mm

17. Very stable, base ventilation state
d = $\frac{1}{4}$ in. = 6.3 mm
U = 5.44 f.p.s. = 1.66 m/sec
H = 0.228 ft = 69.5 mm

18. Transition form
d = $\frac{1}{4}$ in. = 6.3 mm
U = 4.00 f.p.s. = 1.22 m/sec
H = 0.163 ft = 49.7 mm

Fig. 3 continued

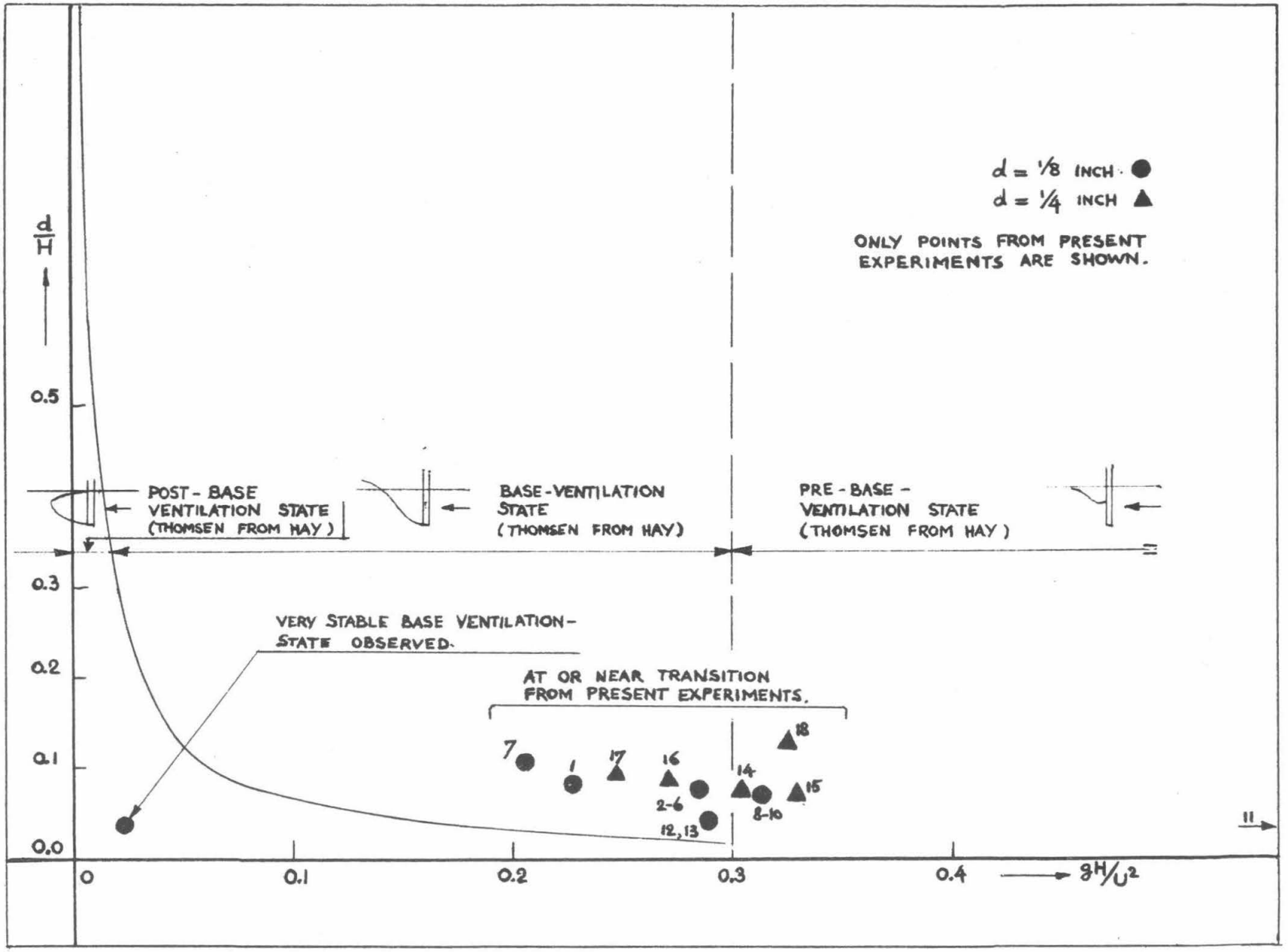

Fig. 4, Position of Experimental Points in Thomsen's Diagram (Fig. 4, Ref. 1)
The numbers shown, refer to the photographs of Fig. 3.

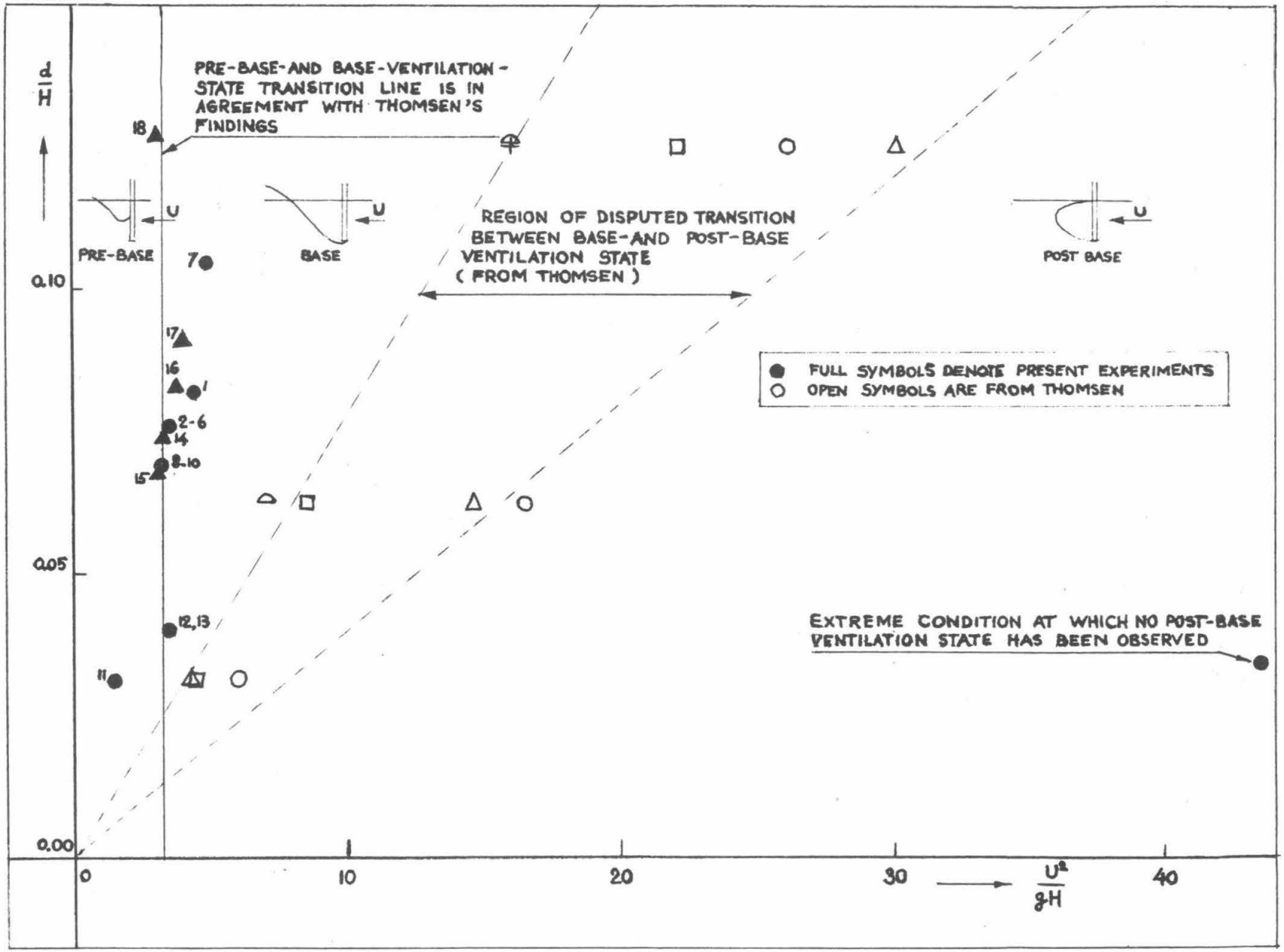

Fig. 5, Diagram of Fig. 4 on Inverted Base. The numbers shown, refer to the photographs of Fig. 3.

DISTRIBUTION LIST FOR UNCLASSIFIED TECHNICAL REPORTS
ISSUED UNDER
CONTRACT Nonr 220(43)
(Single copies unless otherwise specified)

Chief of Naval Research
Department of the Navy
Washington 25, D.C.
Attn: Codes 438 (3)
461
463
466

Commanding Officer
Office of Naval Research
Branch Office
495 Summer Street
Boston 10, Massachusetts

Commanding Officer
Office of Naval Research
Branch Office
207 West 24th Street
New York 11, New York

Commanding Officer
Office of Naval Research
Branch Office
1030 East Green Street
Pasadena, California

Commanding Officer
Office of Naval Research
Branch Office
1000 Geary Street
San Francisco 9, California

Commanding Officer
Office of Naval Research
Branch Office
Box 39, Navy No. 100
Fleet Post Office
New York, New York (25)

Director
Naval Research Laboratory
Washington 25, D. C.
Attn: Code 2027 (6)

Chief, Bureau of Naval Weapons
Department of the Navy
Washington 25, D. C.
Attn: Codes RUAW-r
RRRE
RAAD
RAAD-222
DIS-42

Commander
U. S. Naval Ordnance Test Station
China Lake, California
Attn: Code 753

Chief, Bureau of Ships
Department of the Navy
Washington 25, D. C.
Attn: Codes 310
312
335
420
421
440
442
449

Chief, Bureau of Yards and Docks
Department of the Navy
Washington 25, D. C.
Attn: Code D-400

Commanding Officer and Director
David Taylor Model Basin
Washington 7, D. C.
Attn: Codes 108
142
500
513
520
525
526
526A
530
533
580
585
589
591
591A
700

Commander
U.S. Naval Ordnance Test Station
Pasadena Annex
3202 E. Foothill Blvd.
Pasadena 8, California
Attn: Code P-508

Commander
Planning Department
Portsmouth Naval Shipyard
Portsmouth, New Hampshire

Commander
Planning Department
Boston Naval Shipyard
Boston 29, Massachusetts

Commander
Planning Department
Pearl Harbor Naval Shipyard
Navy No. 128, Fleet Post Office
San Francisco, California

Commander
Planning Department
San Francisco Naval Shipyard
San Francisco 24, California

Commander
Planning Department
Mare Island Naval Shipyard
Vallejo, California

Commander
Planning Department
New York Naval Shipyard
Brooklyn 1, New York

Commander
Planning Department
Puget Sound Naval Shipyard
Bremerton, Washington

Commander
Planning Department
Philadelphia Naval Shipyard
U. S. Naval Base
Philadelphia 12, Pennsylvania

Commander
Planning Department
Norfolk Naval Shipyard
Portsmouth, Virginia

Commander
Planning Department
Charleston Naval Shipyard
U. S. Naval Base
Charleston, South Carolina

Commander
Planning Department
Long Beach Naval Shipyard
Long Beach 2, California

Commander
Planning Department
U. S. Naval Weapons Laboratory
Dahlgren, Virginia

Commander
U. S. Naval Ordnance Laboratory
White Oak, Maryland

Dr. A. V. Hershey
Computation and Exterior
Ballistics Laboratory
U. S. Naval Weapons Laboratory
Dahlgren, Virginia

Superintendent
U. S. Naval Academy
Annapolis, Maryland
Attn: Library

Superintendent
U. S. Naval Postgraduate School
Monterey, California

Commandant
U. S. Coast Guard
1300 E. Street, N. W.
Washington, D. C.

Secretary Ship Structure Committee
U. S. Coast Guard Headquarters
1300 E Street, N. W.
Washington, D. C.

Commander
Military Sea Transportation Service
Department of the Navy
Washington 25, D. C.

U. S. Maritime Administration
GAO Building
441 G Street, N. W.
Washington, D. C.
Attn: Division of Ship Design
Division of Research

Superintendent
U. S. Merchant Marine Academy
Kings Point, Long Island, New York
Attn: Capt. L. S. McCready
(Dept. of Engineering)

Commanding Officer and Director
U. S. Navy Mine Defense Laboratory
Panama City, Florida

Commanding Officer
NROTC and Naval Administrative
Massachusetts Institute of Technology
Cambridge 39, Massachusetts

U. S. Army Transportation Research and
Development Command
Fort Eustis, Virginia
Attn: Marine Transport Division

Mr. J. B. Parkinson
National Aeronautics and Space
Administration
1512 H Street, N. W.
Washington 25, D. C.

Director
Langley Research Center
Langley Station
Hampton, Virginia
Attn: Mr. I. E. Garrick
Mr. D. J. Marten

Director Engineering Sciences Division
National Science Foundation
1951 Constitution Avenue, N. W.
Washington 25, D. C.

Director
National Bureau of Standards
Washington 25, D. C.
Attn: Fluid Mechanics Division
(Dr. G. B. Schubauer)
Dr. G. H. Keulegan
Dr. J. M. Franklin

Defense Documentation Center
Cameron Station
Alexandria, Virginia (20)

Office of Technical Services
Department of Commerce
Washington 25, D. C.

California Institute of Technology
Pasadena 4, California
Attn: Professor M. S. Plesset
Professor T. Y. Wu
Professor A. J. Acosta

University of California
Department of Engineering
Los Angeles 24, California
Attn: Dr. A. Powell

Director
Scripps Institute of Oceanography
University of California
La Jolla, California

Professor M. L. Albertson
Department of Civil Engineering
Colorado A and M College
Fort Collins, Colorado

Professor J. E. Cermak
Department of Civil Engineering
Colorado State University
Fort Collins, Colorado

Professor W. R. Sears
Graduate School of Aeronautical Engineering
Cornell University
Ithaca, New York

State University of Iowa
Iowa Institute of Hydraulic Research
Iowa City, Iowa
Attn: Dr. H. Rouse
Dr. L. Landweber

Massachusetts Institute of Technology
Cambridge 39, Massachusetts
Attn: Department of Naval Architecture
and Marine Engineering
Professor A. T. Ippen

Harvard University
Cambridge 38, Massachusetts
Attn: Professor G. Birkhoff
(Dept. of Mathematics)
Professor G. F. Carrier
(Dept. of Mathematics)

University of Michigan
Ann Arbor, Michigan
Attn: Professor R. B. Couch
(Dept. of Naval Architecture)
Professor W. W. Willmarth
(Aero. Engineering Department)

Dr. L. G. Straub, Director
St. Anthony Falls Hydraulic Laboratory
University of Minnesota
Minneapolis 14, Minnesota
Attn: Mr. J. N. Wetzel
Professor B. Silberman

Professor J. J. Foody
Engineering Department
New York State University Maritime College
Fort Schulyer, New York

New York University
Institute of Mathematical Sciences
25 Waverly Place
New York 3, New York
Attn: Professor J. Keller
Professor J. J. Stoker

The Johns Hopkins University
Department of Mechanical Engineering
Baltimore 18, Maryland
Attn: Professor S. Corrsin
Professor O. M. Phillips (2)

Massachusetts Institute of Technology
Department of Naval Architecture and
Marine Engineering
Cambridge 39, Massachusetts
Attn: Professor M. A. Abkowitz, Head

Dr. G. F. Wislicenus
Ordnance Research Laboratory
Pennsylvania State University
University Park, Pennsylvania
Attn: Dr. M. Sevik

Professor R. C. DiPrima
Department of Mathematics
Rensselaer Polytechnic Institute
Troy, New York

Director
Woods Hole Oceanographic Institute
Woods Hole, Massachusetts

Stevens Institute of Technology
Davidson Laboratory
Castle Point Station
Hoboken, New Jersey
Attn: Mr. D. Savitsky
Mr. J. P. Breslin
Mr. C. J. Henry
Mr. S. Tsakonas

Webb Institute of Naval Architecture
Crescent Beach Road
Glen Cove, New York
Attn: Professor E. V. Lewis
Technical Library

Executive Director
Air Force Office of Scientific Research
Washington 25, D. C.
Attn: Mechanics Branch

Commander
Wright Air Development Division
Aircraft Laboratory
Wright-Pattern Air Force Base, Ohio
Attn: Mr. W. Mykytow, Dynamics Branch

Cornell Aeronautical Laboratory
4455 Genesee Street
Buffalo, New York
Attn: Mr. W. Targoff
Mr. R. White

Massachusetts Institute of Technology
Fluid Dynamics Research Laboratory
Cambridge 39, Massachusetts
Attn: Professor H. Ashley
Professor M. Landahl
Professor J. Dugundji

Hamburgische Schiffbau-Versuchsanstalt
Bramfelder Strasse 164
Hamburg 33, Germany
Attn: Dr. H. Schwanecke
Dr. H. W. Lerbs

Institut fur Schiffbau der Universitat Hamburg
Berliner Tor 21
Hamburg 1, Germany
Attn: Prof. G. P. Weinblum

Transportation Technical Research Institute
1-1057, Mejiro-Cho, Toshima-Ku
Tokyo, Japan

Max-Planck Institut fur Stromungsforschung
Bottingerstrasse 6/8
Gottingen, Germany
Attn: Dr. H. Reichardt

Hydro-og Aerodynamisk Laboratorium
Lyngby, Denmark
Attn: Professor Carl Prohaska

Shipsmodelltanken
Trondheim, Norway
Attn: Professor J. K. Lunde

Versuchsanstalt fur Wasserbau and Schiffbau
Schleuseninsel im Tiergarten
Berlin, Germany
Attn: Dr. S. Schuster, Director
Dr. Grosse

Technische Hogeschool
Institut voor Toegepaste Wiskunde
Julianalaan 132
Delft, Netherlands
Attn: Professor R. Timman

Bureau D'Analyse et de Recherche Appliquees
47 Avenue Victor Bresson
Issy-Les-Moulineaux
Seine, France
Attn: Professor Siestrunck

Netherlands Ship Model Basin
Wageningen, The Netherlands
Attn: Dr. Ir. J. D. vanManen

National Physical Laboratory
Teddington, Middlesex, England
Attn: Mr. A. Silverleaf, Superintendent Ship Division
Head, Aerodynamics Division

Head, Aerodynamics Department
Royal Aircraft Establishment
Farnborough, Hants, England
Attn: Mr. M. O. W. Wolfe

Dr. S. F. Hoerner
148 Busteed Drive
Midland Park, New Jersey

Boeing Airplane Company
Seattle Division
Seattle, Washington
Attn: Mr. M. J. Turner

Electric Boat Division
General Dynamics Corporation
Groton, Connecticut
Attn: Mr. Robert McCandliss

General Applied Sciences Labs., Inc.
Merrick and Stewart Avenues
Westbury, Long Island, New York

Gibbs and Cox, Inc.
21 West Street
New York, New York

Lockheed Aircraft Corporation
Missiles and Space Division
Palo Alto, California
Attn: R. W. Kermeen

Grumman Aircraft Engineering Corp.
Bethpage, Long Island, New York
Attn: Mr. E. Baird
Mr. E. Bower
Mr. W. P. Carl

Midwest Research Institute
425 Volker Blvd.
Kansas City 10, Missouri
Attn: Mr. Zeydel

Director, Department of Mechanical Sciences
Southwest Research Institute
8500 Culebra Road
San Antonio 6, Texas
Attn: Dr. H. N. Abramson
Mr. G. Ransleben
Editor, Applied Mechanics Review

Convair
A Division of General Dynamics
San Diego, California
Attn: Mr. R. H. Oversmith
Mr. H. T. Brooke

Hughes Tool Company
Aircraft Division
Culver City, California
Attn: Mr. M. S. Harned

Hydronautics, Incorporated
Pindell School Road
Howard County
Laurel, Maryland
Attn: Mr. Phillip Eisenberg

Rand Development Corporation
13600 Deise Avenue
Cleveland 10, Ohio
Attn: Dr. A. S. Iberall

U. S. Rubber Company
Research and Development Department
Wayne, New Jersey
Attn: Mr. L. M. White

Technical Research Group, Inc.
Route 110
Melville, New York, 11749
Attn: Mr. Jack Kotik

Mr. C. Wigley
Flat 102
6-9 Charterhouse Square
London, E. C. 1, England

AVCO Corporation
Lycoming Division
1701 K Street, N. W.
Apt. No. 904
Washington, D. C.
Attn: Mr. T. A. Duncan

Mr. J. G. Baker
Baker Manufacturing Company
Evansville, Wisconsin

Curtiss-Wright Corporation Research Division
Turbomachinery Division
Quehanna, Pennsylvania
Attn: Mr. George H. Pedersen

Dr. Blaine R. Parkin
AiResearch Manufacturing Corporation
9851-9951 Sepulveda Boulevard
Los Angeles 45, California

The Boeing Company
Aero-Space Division
Seattle 24, Washington
Attn: Mr. R. E. Bateman
(Internal Mail Station 46-74)

Lockheed Aircraft Corporation
California Division
Hydrodynamics Research
Burbank, California
Attn: Mr. Bill East

National Research Council
Montreal Road
Ottawa 2, Canada
Attn: Mr. E. S. Turner

The Rand Corporation
1700 Main Street
Santa Monica, California
Attn: Technical Library

Stanford University
Department of Civil Engineering
Stanford, California
Attn: Dr. Byrne Perry
Dr. E. Y. Hsu

Dr. Hirsh Cohen
IBM Research Center
P. O. Box 218
Yorktown Heights, New York

Mr. David Wellinger
Hydrofoil Projects
Radio Corporation of America
Burlington, Massachusetts

Food Machinery Corporation
P. O. Box 367
San Jose, California
Attn: Mr. G. Tedrew

Dr. T. R. Goodman
Oceanics, Inc.
Technical Industrial Park
Plainview, Long Island, New York

Professor Brunelle
Department of Aeronautical Engineering
Princeton University
Princeton, New Jersey

Commanding Officer
Office of Naval Research Branch Office
230 N. Michigan Avenue,
Chicago 1, Illinois

University of Colorado
Aerospace Engineering Sciences
Boulder, Colorado
Attn: Prof. M. S. Uberoi

The Pennsylvania State University
Dept. of Aeronautical Engineering
Ordnance Research Laboratory
P. O. Box 30
State College, Pennsylvania
Attn: Professor J. William Holl

Institut fur Schiffbau der Universitat Hamburg
Lammersieth 90
2 Hamburg 33, Germany
Attn: Dr. O. Grim